Diurnal variations of circulation and precipitation in the vicinity of the Tibetan Plateau in early summer

K. C. Chow · Johnny C. L. Chan

Abstract A regional climate model (RCM) has been applied to simulate the diurnal variations of the Asian summer monsoon during the early summer period. The ERA40 reanalysis data and the TRMM precipitation data are used to evaluate the performance of the model. The 5-year simulations show that the RCM could simulate well the diurnal cycle of the monsoon circulation over the region. A strong diurnal variation of circulation over the Tibetan Plateau (TP) can be observed at the 500-hPa level, with strong convergence and upward motion in the late afternoon. The diurnal variation of the 500-hPa relative vorticity over the TP associated with the corresponding diurnal variation of convergence may lead to the formation of a prominent plateau-scale cyclonic circulation over the TP during the evening to midnight period. The simulated diurnal variation of precipitation over land is generally better than that over the ocean, particularly over the regions close to the TP such as the Bangladesh region in the southern flank of the TP, where the well-known nocturnal maximum in precipitation is well captured by the RCM. However, the late-afternoon maximum in precipitation over the Southeast Asia region is not well simulated by the RCM. The model results suggest that the diurnal variation of precipitation over the southern flank of the TP is associated with the strong diurnal variation in the circulation over the TP.

1 Introduction

The diurnal variation of precipitation in tropical regions has been studied by numerous researches (e.g. Nitta and Sekine 1994; Johnson et al. 2001; Ohsawa et al. 2001; Yang and Slingo 2001; Nesbitt and Zipser 2003; Hirose and Nakamura 2005). These studies suggested a maximum precipitation over land and oceanic regions during the periods of late afternoon and early morning respectively with small seasonal variation. The diurnal variation of precipitation over the Southeast Asian regions generally follows this regime. However, in some regions a nocturnal maximum in precipitation is prevalent, such as the Sichuan region in southwest China (Zhang and Lin 1992) and the Bangladesh region (BR) (Bhatt and Nakamura 2005). The latter region is situated in the foothills in the southern slope of the Tibetan Plateau (TP), and has a large precipitation rate in summer due to the strong southwesterlies associated with the Asian summer monsoon (ASM). The strong diurnal variation of precipitation over BR has received considerable attention in recent years (e.g. Barros and Lang 2003; Bhatt and Nakamura 2005, 2006; Islam et al. 2005; Kataoka and Satomura 2005). These studies suggested that the nocturnal maximum in precipitation over the BR is associated with the southward shift of the precipitation zone from the ridge in the late afternoon to the foothills in the early morning along the southern slope of the TP.

K. C. Chow · J. C. L. Chan
CityU-IAP Laboratory for Atmospheric Sciences,
Department of Physics and Materials Science,
City University of Hong Kong, Hong Kong, China

K. C. Chow (✉)
Atmospheric Research Center,
HKUST Fok Ying Tung Graduate School,
Hong Kong University of Science and Technology,
Nansha IT Park, Nansha, Guangzhou, China
e-mail: kchow@ust.hk

While regimes of precipitation diurnal cycle have been identified in some regions, the mechanisms behind the observed patterns are not clearly understood. In general, the diurnal variation of precipitation is associated with the corresponding diurnal variation of the circulation. However, relatively few studies have been performed on the diurnal variation of the circulation. With the Asian continent having such a large spatial variation in topography, especially the huge elevated TP, as well as a complex land-sea distribution, the mechanisms responsible for the diurnal variations of circulation and precipitation should also be complicated.

The TP is well recognized for its influence on the diurnal variation of circulation over the Asian continent. Krishnamurti and Kishtawal (2000) pointed out that in the summer, a continent-scale diurnal variation of the circulation can be observed over the TP in the upper troposphere. The wide impact of the TP on the diurnal cycle of the circulation is clear that its effect can even be observed in a simple numerical simulation of the diurnal cycle over the TP (Kuo and Qian 1981). In their pioneer numerical study, they used a coarse resolution "dry" model (no precipitation) with only five vertical levels. Based on the analysis of the reanalysis data at 00 UTC and 12 UTC, Yanai et al. (1992) and Yanai and Li (1994) found significant diurnal variations of vertical motion, surface temperature, and convective activities over the TP during the summer period. Their results also revealed a large-scale diurnal variation of the circulation around the TP, as well as strong and weak vertical motion and convective activities over the TP in the evening (12 UTC) and morning (00 UTC) respectively. Strong and weak convective activities during these two periods are also supported by some recent observational studies over the TP (e.g. Yanai and Li 1994; Ueno et al. 2001; Fujinami and Yasunari 2001; Liu et al. 2002).

One objective of this study is to investigate the capability of a regional climate model (RCM) in simulating the diurnal variations of circulation and precipitation in the East Asian region during the early summer period. The high resolution simulations by the RCM may help understand the mesoscale dynamics of the diurnal cycle in regions with complex topographies, particularly those in the TP vicinity such as BR. This study focuses on the mean diurnal cycle in June, which is the period when the Tibetan High of the ASM is established in the upper troposphere over the TP, and the Mei-yu rainband is well established along southern China, the Yangtze River region, and Japan. Examining the results of this month may help understand the diurnal cycles of these monsoon phenomena. In fact, exceptionally large Meiyu precipitation over the Yangtze River region has been related to the generation of the southwest or Sichuan vortices (Tao and Ding 1981) at the

eastern flank of the TP, which in turn may be related to the diurnal cycle of convective activities over the TP (Yasunari and Miwa 2006).

A brief description of the RCM and the details of the simulations will be introduced in Section 2. In Section 3, the performance of the RCM in simulating the diurnal cycles of precipitation and circulation in the Asian region will be evaluated. Some general features of the diurnal cycles of circulation and precipitation in the region will also be discussed. Section 4 will focus on the diurnal variation of the circulation over the TP and its vicinity. The mechanism responsible for the nocturnal maximum in precipitation over the southern flank of the TP will also be discussed in this section. The results of this study will be summarized in Section 5.

2 The numerical simulations

The regional climate model used in this study is a modified version of the NCAR RegCM2 (Giorgi et al. 1993a, b). Some details of the RCM have been described in Chan et al. (2004) and Chow et al. (2006). The model domain without the buffer zone for the lateral boundary conditions is shown in Fig. 1. The RCM used in this study has 20 vertical levels and a 60-km horizontal resolution. The Anthes-Kuo cumulus convection parameterization scheme (Anthes 1977; Anthes et al. 1987) is adopted to simulate the cumulus precipitation. The initial and lateral boundary conditions of the atmosphere are from the European Centre for Medium-Range Weather Forecast (ECMWF) ERA40
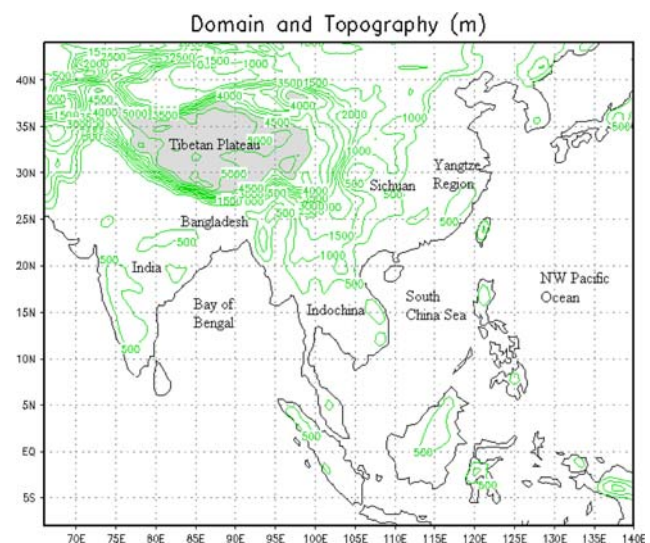

Fig. 1 Domain of the numerical simulations with the buffer zone excluded. The *contours* show the topography at 500 m interval and the *shaded* region depicts the region of the Tibetan Plateau with topography over 4,500 m. Also shown are the names of some places mentioned in this study

reanalyses, and the sea-surface temperature (SST) data are the Optimum Interpolation SST V2 weekly mean data obtained from the Climate Diagnostics Center of the US National Oceanic and Atmospheric Administration.

The performance of the RCM is evaluated using the precipitation data of the tropical rainfall measuring mission (TRMM), obtained from the National Aeronautics and Space Administration. The data set 3B42 version 6 of TRMM has been used in this study, which has a 0.25° × 0.25° resolution and outputs at 3 h interval at 00, 03, 06, 09, 12, 15, 18, 21 UTC. Because the availability of the TRMM data is from 1998 to present and the reanalysis data ERA40 for the lateral boundary conditions of the RCM is available up to 2002, the 5 years from 1998 to 2002 were chosen for the RCM simulations.

Five simulations for each of the 5 years from 1998 to 2002 have been performed by the RCM. In each simulation, the integration is from 1 April to 30 June. Eight outputs from 00 to 21 UTC are generated for each day at a 3 h interval. The 5 years mean diurnal cycle is obtained from the arithmetic mean of the results for these 5 years. In this study, diurnal variations are interpreted as the anomalies from the daily averaged fields. The daily averaged values are calculated by averaging the eight daily outputs.

2.1 Simulations of the daily-mean fields

The model results show that the RCM is capable of simulating the pattern as well as the quantity of the 5 years mean total precipitation in June (Fig. 2). In particular, the major precipitation zones in China, such as those in southern China and the Yangtze River region (115°–120°E, 25°–30°N), can be captured by the model (Fig. 2a, b). In addition, the Meiyu rainband over eastern China and Japan, which is a distinct feature of the ASM in June, can also be well simulated. The RCM could also simulate the precipitation associated with the Indian summer monsoon, such as the major precipitation zones over the western coast of India and the Bay of Bengal.

The RCM is also capable of simulating the circulation of the ASM in June. The simulated monthly-mean velocity fields at levels 850, 500, and 200 hPa (Fig. 3a, c, e) are generally comparable with those from the ERA40 data (Fig. 3b, d, f). Some major circulations of the ASM can be identified from the model simulations. In the lower troposphere, the strong southwesterly flow of the Somali jet over India and the BOB region and the anticyclonic flow associated with the North Western Pacific anticyclone can be captured by the model (Fig. 3a–d). In the upper troposphere, the prominent anticyclonic flow over the TP associated with the Tibetan High (Fig. 3e, f) can also be well simulated.
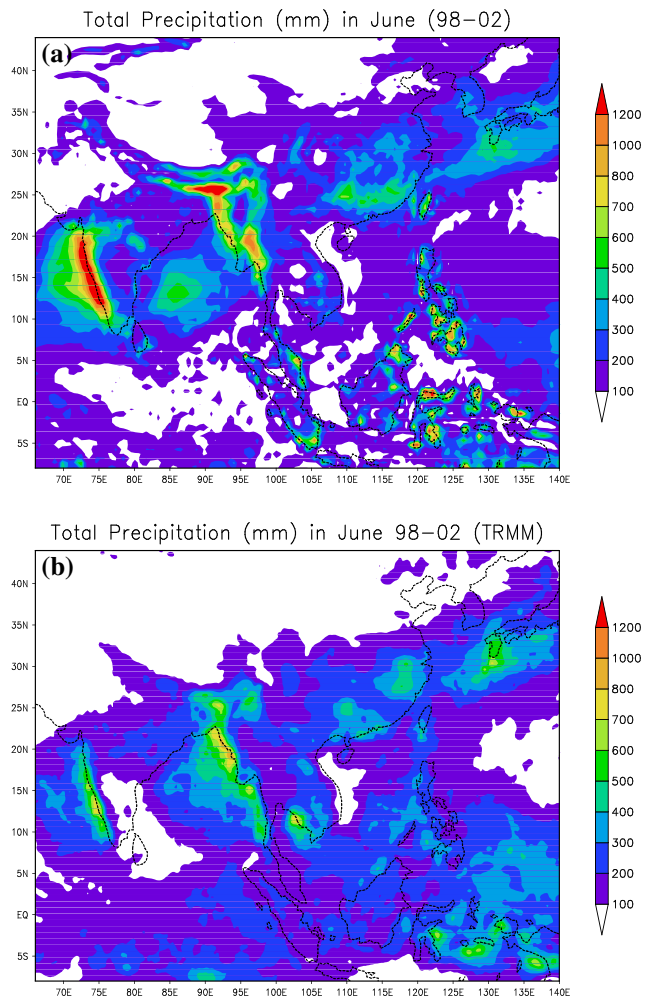

Fig. 2 Total precipitation (mm) in June averaged for the years 1998–2002. **a** Model simulations. **b** TRMM data

3 Diurnal cycles simulated by the RCM

3.1 Diurnal variation of precipitation

Although the RCM can successfully simulate the total precipitation in June, the simulation of the diurnal variation (Fig 4a, c, e, g, i, k, m, o) is generally not as good when compared with the corresponding TRMM data (Fig. 4b, d, f, h, j, l, n, p). In particular, the late afternoon maximum of precipitation over the Southeast Asian region reported in many studies (e.g. Nitta and Sekine 1994; Ohsawa et al. 2001) cannot be captured by the model. The maximum precipitation over the Southeast Asian region (e.g. Indochina and Malaysian Peninsulas) is at 12 UTC in the TRMM data (Fig. 4j), while it is at about 18 UTC in the model simulation (Fig. 4k, m). The TRMM data also shows a maximum in precipitation over southeast China at 09 UTC (Fig. 4h), which could not be reproduced by the model. The diurnal variation of precipitation averaged over
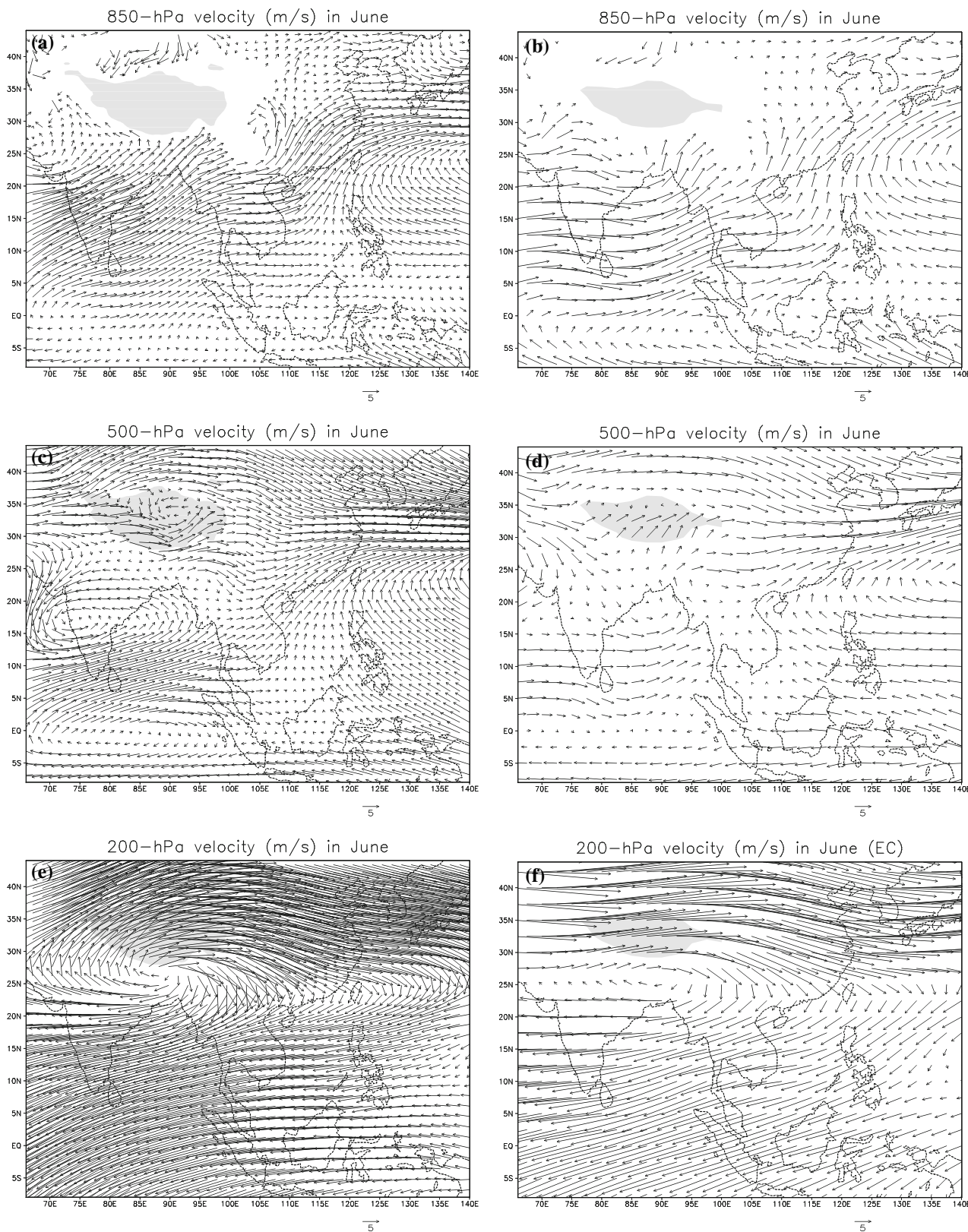
Fig. 3 Monthly mean velocity fields (m s^{-1}) in June averaged for the years 1998–2002 at levels **a**, **b** 850 hPa with values not shown in the regions with topography over 1,500 m, **c**, **d** 500 hPa, and **e**, **f** 200 hPa. **a**, **c**, **e** are model simulations, while **b**, **d**, **f** are ERA40 data. *Shadings* show the Tibetan Plateau with topography over 4,500 m
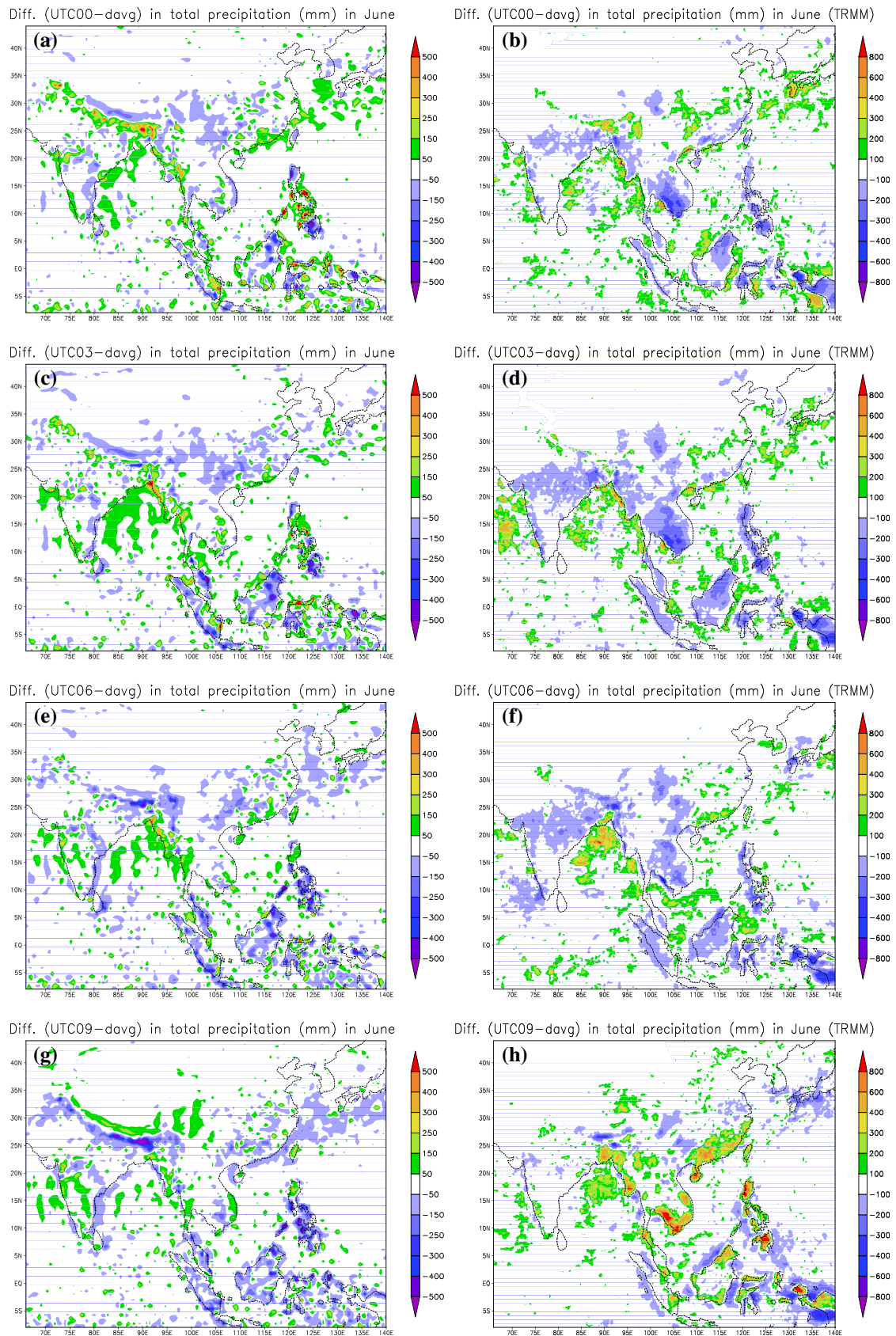
Fig. 4 Diurnal variations (00, 03, 06, 09, 12, 15, 18, 21 UTC minus daily mean) of total precipitation (mm) in June for the years 1998–2002. **a**, **c**, **e**, **g**, **i**, **k**, **m**, **o** are model simulations, and **b**, **d**, **f**, **h**, **j**, **l**, **n**, **p** are TRMM data
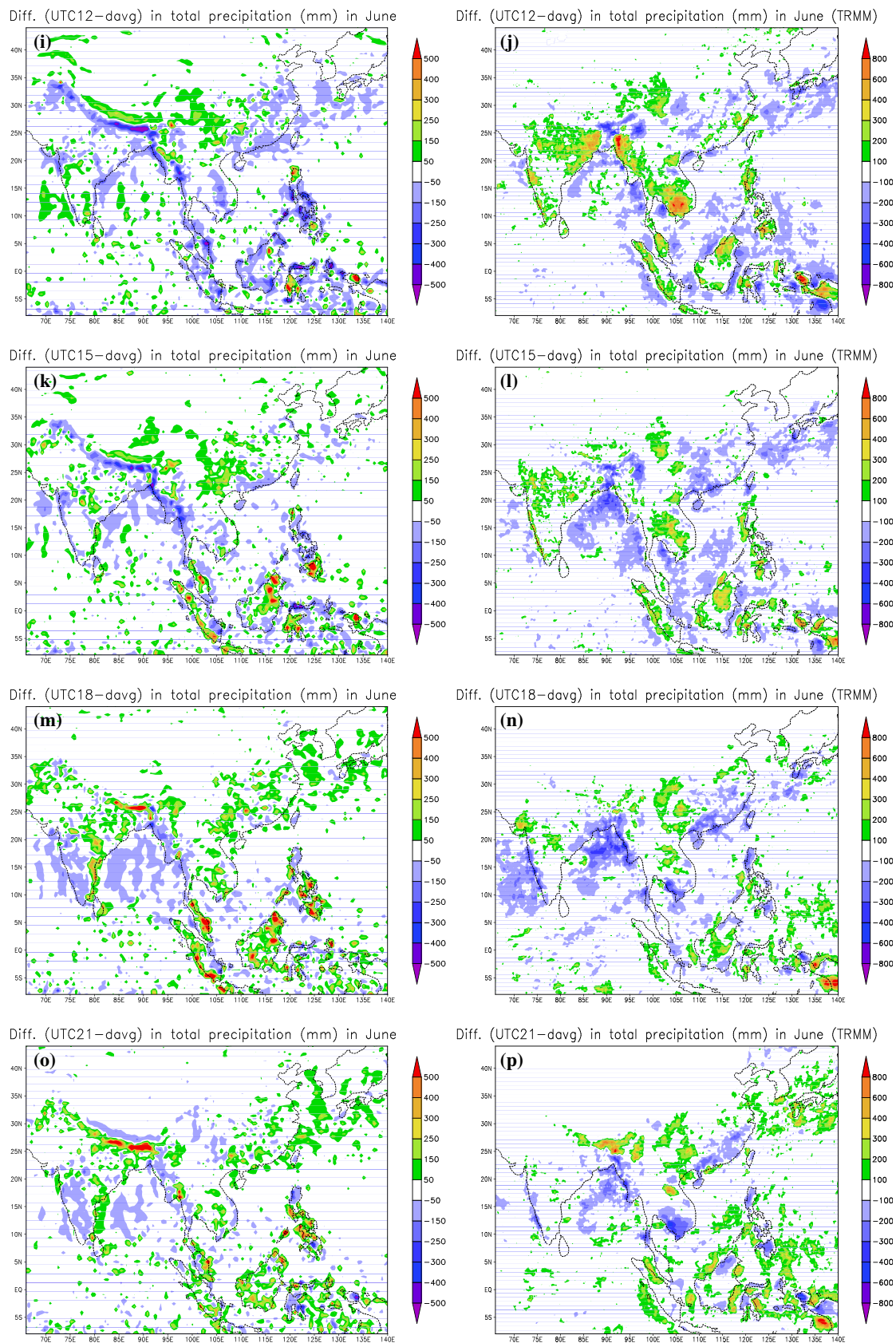
Fig. 4 continued

the Indochina Peninsula (Fig. 5a) shows a single maximum in precipitation in the late afternoon between 09 and 12 UTC in the TRMM data, but a double maximum in the morning to early afternoon period (03 to 09 UTC) and midnight (18 UTC) in the model results.

On the other hand, the diurnal cycle of precipitation in some regions can be successfully captured by the model. The one of particular interest is the nocturnal maximum in precipitation over the southern flank of the TP (Fig. 4o, p) and the subsequent southward shift to the BOB region in the morning from 00 to 06 UTC (Fig. 4a–f). This precipitation pattern has been reported in many studies (e.g. Krishnamurti and Kishtawal 2000; Barros and Lang 2003; Bhatt and Nakamura 2005, 2006; Islam et al. 2005), and is likely associated with the diurnal variation of circulation around the TP. The mechanism responsible for this

precipitation pattern will be further discussed in Section 4.2 based on the model results. In fact, it can be observed from Fig. 5b that the RCM is capable of simulating the diurnal variation of precipitation over BR (88°–92°E, 25°–27°N), with the maximum at 21 UTC and the minimum at about 12 UTC.

The Sichuan region (103°–108°E, 27°–32°N) in southwest China is well known for its nocturnal rain. This precipitation trend can also be captured by the RCM (Fig. 5c), although the maximum is around midnight (15 UTC) instead of early morning (21 UTC) in the TRMM data. It can be observed from the model results that the precipitation zone over the Sichuan region is apparently propagating eastward towards the coastal region of China from 12 to 00 UTC (Fig. 4i, k, m, o, a). This precipitation pattern has been pointed out by Hirose and Nakamura
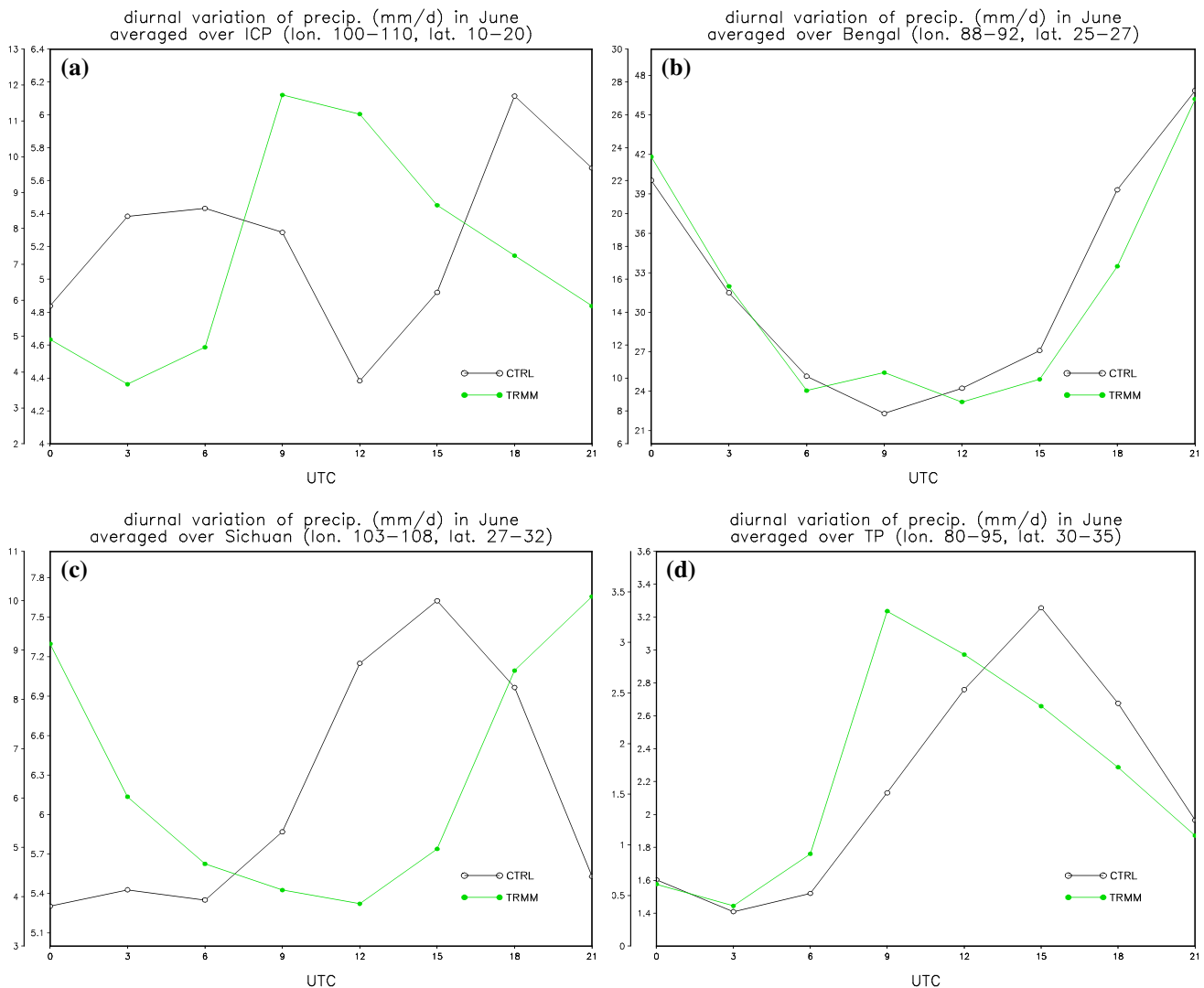

Fig. 5 Diurnal variations of precipitation (mm/day) averaged over **a** The Indochina Peninsula region (100°–110°E, 10°–20°N). **b** The Bangladesh region (88°–92°E, 25°–27°N). **c** The Sichuan region (103°–108°E, 27°–32°N). **d** The central Tibetan Plateau region (80°–95°E, 30°–35°N). *Circles* and *dots*, *right* and *left vertical axes* denote the results from the model and TRMM respectively

(2005), and can also be observed from the TRMM data in Fig. 4. However, similar to the results in Fig. 5c, the time period is shifted for about 6 h from about 18 to 06 UTC (Fig. 4n, p, b, d, f).

The diurnal variation of precipitation averaged over the central TP region (Fig. 5d) shows that the RCM can capture the period of minimum precipitation in the early morning (about 03 UTC). However, the period of maximum precipitation simulated by the RCM is later (at about 15 UTC) than that of the TRMM data (at about 09 UTC). The late afternoon maximum in precipitation over the TP is well known and has been reported in many observational studies (e.g. Ueno et al. 2001; Fujinami and Yasunari 2001; Liu et al. 2002). In general, these studies suggest that the period with maximum precipitation over the TP is in the late afternoon at about 12 UTC.

3.2 Diurnal variation of the circulation

In general, the pattern of the diurnal variation of the circulation is well simulated by the RCM compared with that of the ERA40 data (Figs. 6, 7, 8). The anomalous flow fields show that the diurnal variation of the circulation over land is generally stronger than that over the ocean. The anomalous flow fields at the 850-hPa level (Fig. 6) show a prominent diurnal variation in direction, with an apparent clockwise rotation of 90° for every 6 h. An apparent large land-sea breeze system can be observed from the low-level anomalous field. At 12 UTC (Fig. 6e), the anomalous flow is pointing towards the TP from the coastal region of China, while at 00 UTC (Fig. 6a) the anomalous flow is going out from the TP to the coastal region. Over the coastal region of East Asia, the anomalous 850-hPa flow is northeasterly at 06 UTC (Fig. 6c), while it is southwesterly at 18 UTC (Fig. 6g). These anomalous northeasterly and southwesterly low-level flows may respectively weaken and enhance the prevailing southwesterly monsoonal flow, and may be responsible for the corresponding minimum and maximum of precipitation over the coastal region of East Asia at 06 UTC (Fig. 4e) and 18 UTC (Fig. 4m).

At the 500-hPa level, a prominent diurnal variation in the circulation over the TP can be observed in both the model results and the ERA40 data (Fig. 7). At 00 UTC, a clear anomalous divergent flow occurs over the TP (Fig. 7a). This is the early morning period in the TP region, when the surface temperature over the TP is low. In the counterpart, when the surface temperature is high in the late afternoon of TP at 12 UTC (Fig. 7e), a clear anomalous convergent flow is found over the TP. Between these two periods, anomalous anticyclonic and cyclonic circulations can be observed over the TP at 06 UTC (Fig. 7c) and 18 UTC (Fig. 7g) respectively. The occurrence of

these anomalous anticyclonic and cyclonic circulations is interesting and their formation mechanisms will be further discussed in Section 4.1.

The diurnal variation of the circulation is also strong at the 200-hPa level (Fig. 8). In particular, the divergent and convergent patterns of anomalous flow fields can still be identified over the TP at 00 UTC (Fig. 8a) and 12 UTC (Fig. 8e).

In summary, the model results show that the RCM is capable of simulating the diurnal variation of the circulation, although the diurnal variation of the circulation over the oceanic region simulated by the RCM is generally weaker than that of the ERA40 data. This may be due to the absence of diurnal variation of the SST used by the RCM as the lower boundary condition. Overall, the patterns of the anomalous flow fields suggest that the diurnal variation of the circulations over China, East Asia, and the Indian Peninsula are closely related to the diurnal forcing generated by the TP, as pointed out in some early studies such as Yanai and Li (1994) and Krishnamurti and Kishtawal (2000).

4 Diurnal variation of the circulation in the vicinity of the Tibetan Plateau

In this section the diurnal variation of the circulation around the TP simulated by the RCM is examined more closely. The daily-mean vertical velocity profile in the latitude–altitude cross-section at 90°E (Fig. 9a) shows that upward motion is strong (up to 20 hPa h^{-1}) in the southern flank of the TP. It is worth-noting that this strong upward motion does not originate from the southern slope of the TP, but is originated at the southern edge near the foot of the TP. Apart from this maximum upward motion, moderate upward flow along the southern slope of the TP can be observed (Fig. 9a). This may be an orographic upslope flow basically driven by the terrain-enhanced upward motion when the prevailing low-level southwesterly of the Indian summer monsoon impinging on the southern flank of the TP. The strong precipitation over the BR (Fig. 2) may also enhance the strong upward flow at the southern foot of the TP as mentioned above. It can be observed from the contours of the vertical velocity at the 500-hPa level (Fig. 9b) that the maximum upward motion is in the BR between 90° and 95°E, and is generally coincident with the maximum precipitation zone over there (Fig. 2).

The anomalous circulations in the 90°E latitude–altitude cross-section at the four time periods 00, 06, 12, 18 UTC (Fig. 10) show that the diurnal variation of the vertical motion over the TP and the previous mentioned BR are strong. In these four time periods, the strongest and weakest upward motion over the BR is at 00 UTC

Fig. 6 Diurnal variations (00, 06, 12, 18 UTC minus daily mean) of 850-hPa velocity field (m s^{-1}) in June for the years 1998–2002. **a**, **c**, **e**, **g** are model simulations, and **b**, **d**, **f**, **h** are ERA40 data. *Shadings* show the Tibetan Plateau with topography over 4,500 m
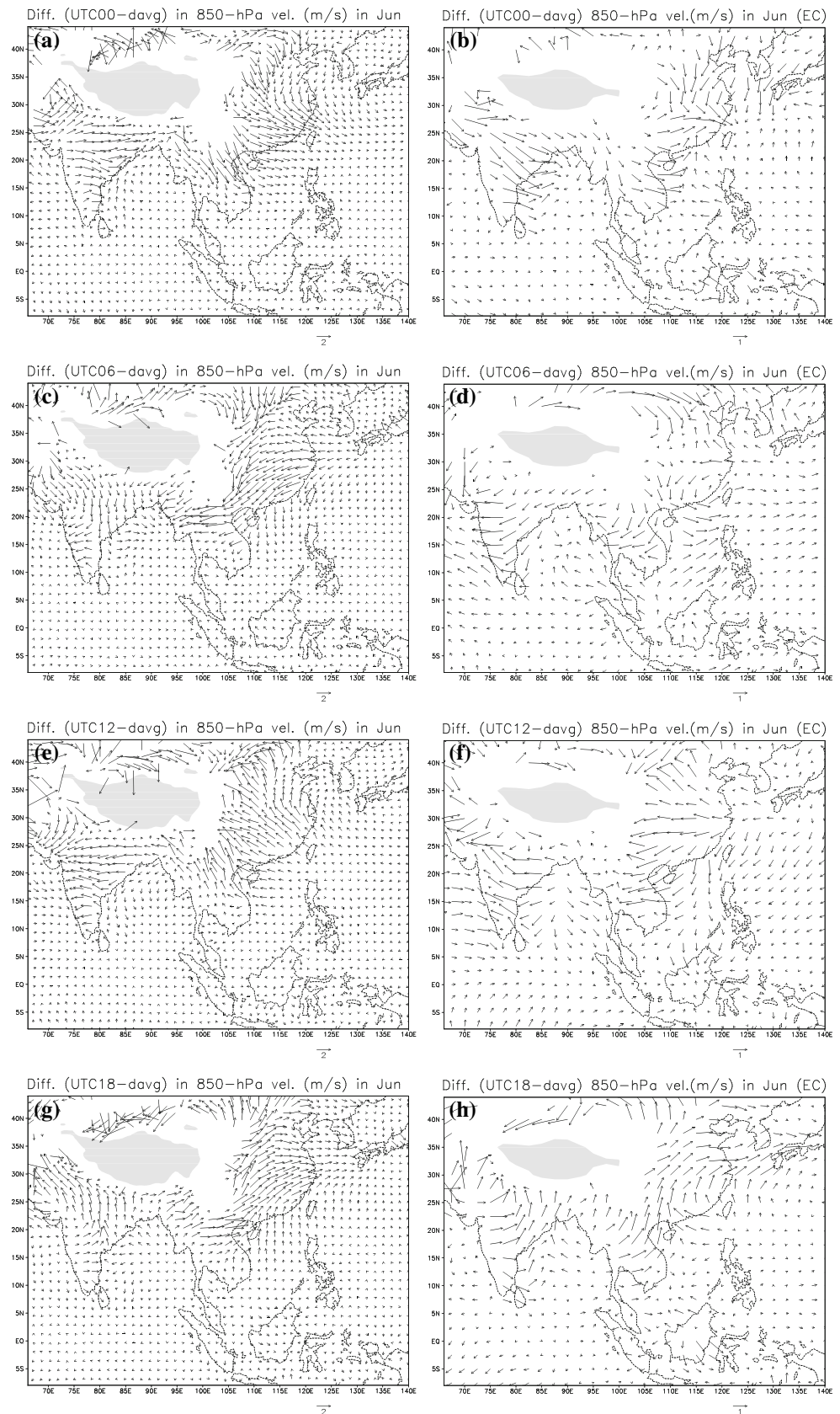
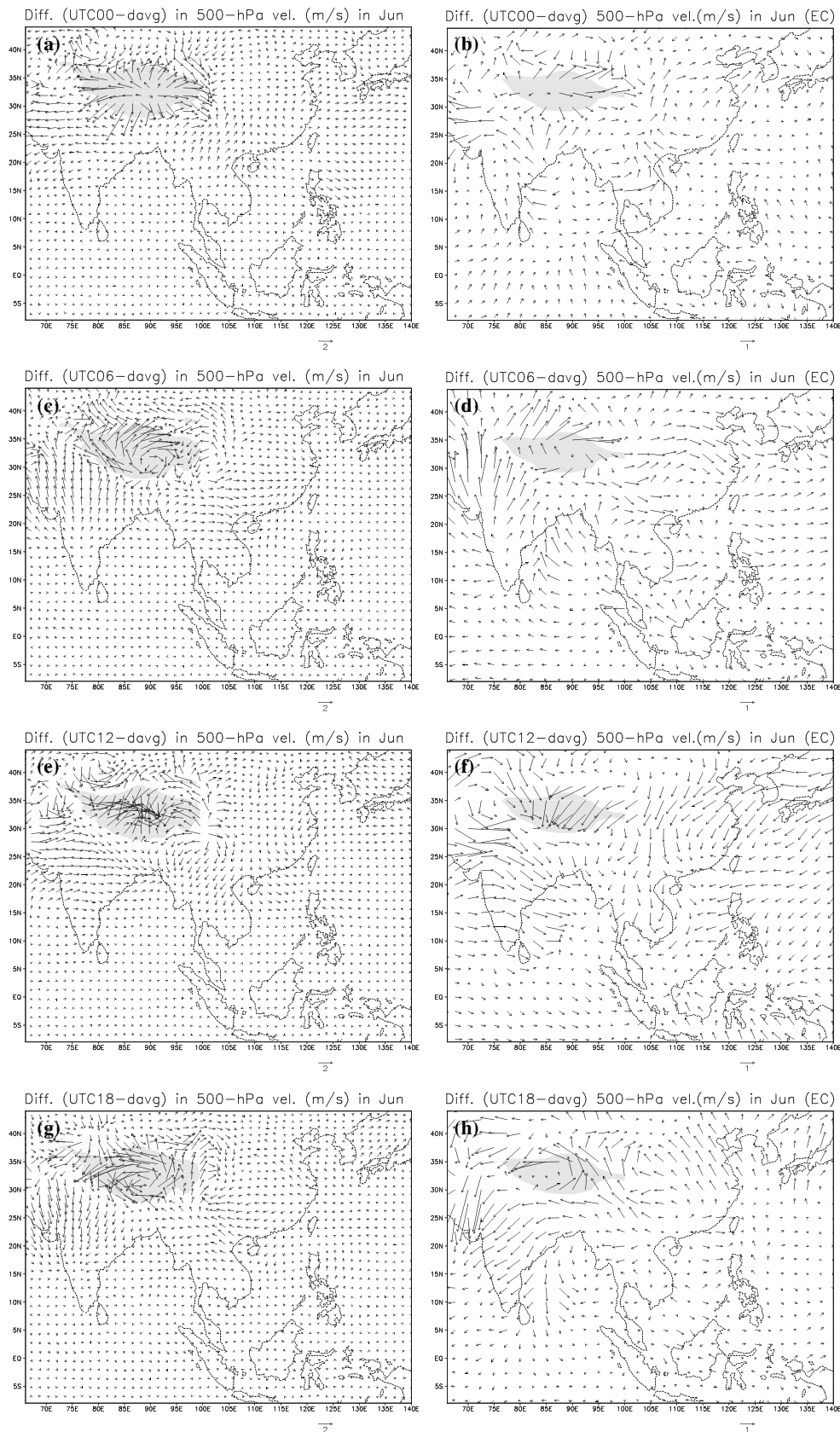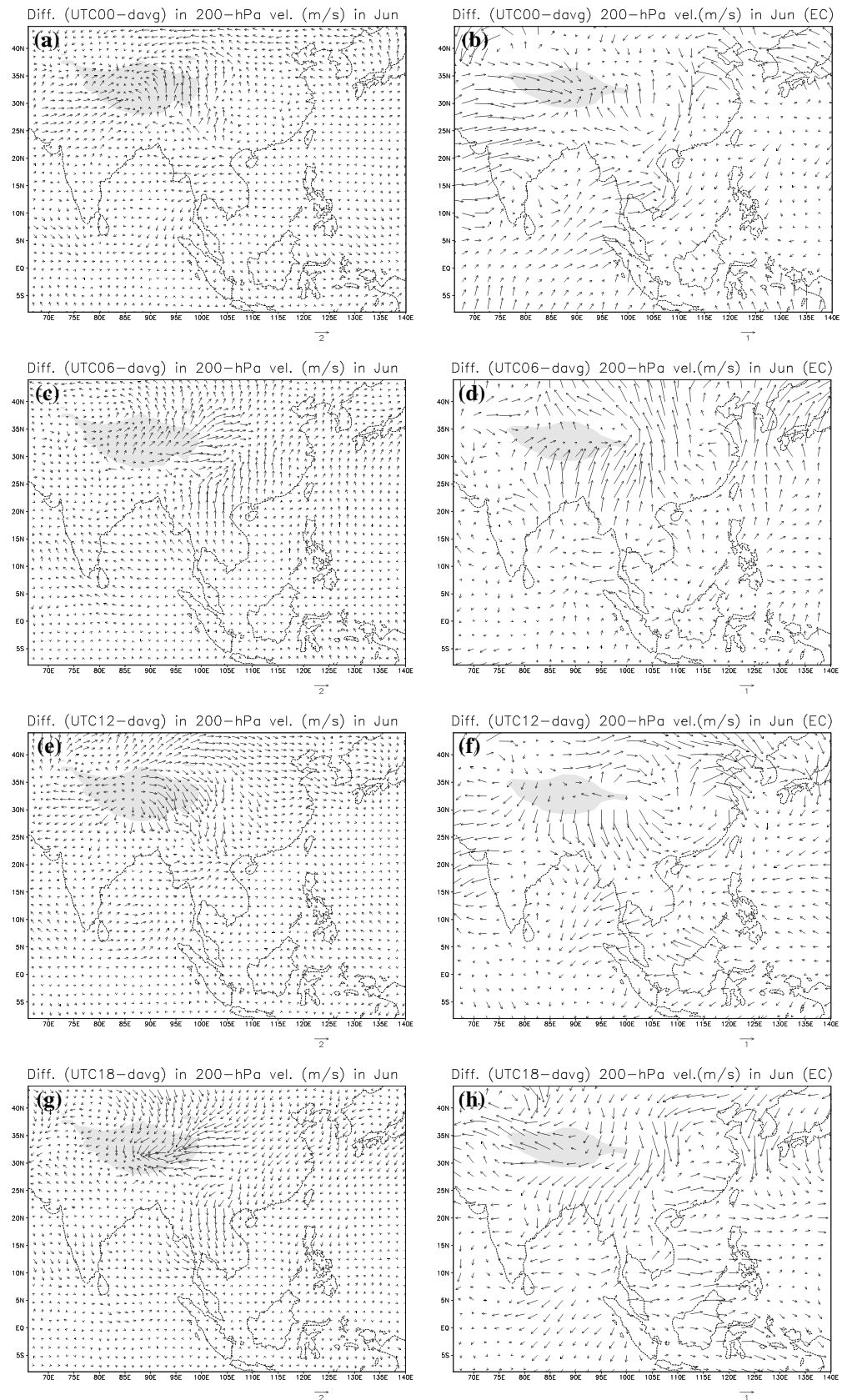**Fig. 7** As in Fig. 6 but for the 500-hPa level

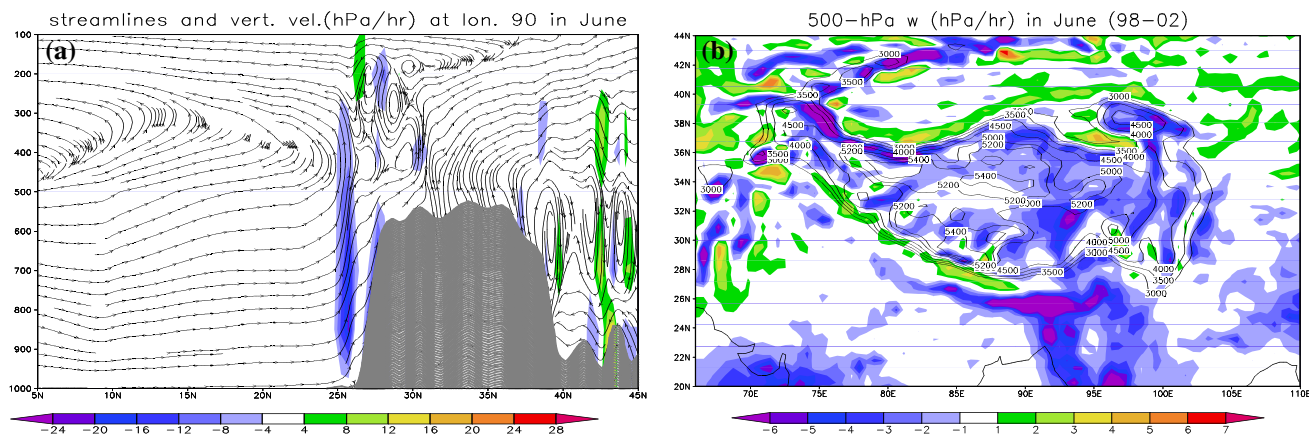**Fig. 8** As in Fig. 6 but for the 200-hPa level

Fig. 9 Vertical velocity (hPa h^{-1}) averaged in June for the years 1998–2002. **a** Vertical velocity (*shadings*) and *streamlines* in the altitude-latitude section at 90°E. **b** At the 500-hPa level with *contours* depicting the topography of the Tibetan Plateau above 3,000 m at 500 m interval

(Fig. 10a, b) and 12 UTC (Fig. 10e, f) respectively. The variation in vertical motion over the TP is in opposite phase with that over the BR, with the strongest and weakest upward motion at 12 UTC and 00 UTC respectively. Similar to the corresponding daily mean field (Fig. 9a), the diurnal variation of the vertical motion over the BR is deep into the upper troposphere at the 300-hPa level. The horizontal distributions of the 500-hP anomalous vertical velocity at the four time periods (Fig. 11) show that significant diurnal variation of vertical motion is not only in the BR region at 90°E, but is in a belt shape at the southern flank of the TP similar to that of the daily mean field (Fig. 9b).

The vertical profiles of the anomalous circulation around the TP (Fig. 10) further illustrate the interesting patterns of anomalous circulations over the TP (Fig. 7) discussed in Section 3.2. In particular, the significant anomalous 500-hPa divergent and convergent flows over the TP respectively at 00 UTC (Fig. 7a) and 12 UTC (Fig. 7e) can be observed in the corresponding vertical profiles (Fig. 10a, b, e, f). These divergent and convergent flows are shallow and confined within the 400 and 500 hPa levels, and the streamlines (Fig. 10b, f) show that these flows are generally associated with the corresponding anomalous downward and upward motions over the TP.

The anomalous 500-hPa anticyclonic and cyclonic circulations over the TP at 06 UTC (Fig. 7c) and 18 UTC (Fig. 7g) can also be observed from the anomalous zonal wind over the TP in the corresponding vertical sections (Fig. 10d, h). Similar to the anomalous divergent and convergent flows at 00 UTC and 12 UTC, these anomalous anticyclonic and cyclonic circulations are also shallow and confined within the 400 and 500 hPa levels.

A strong anomalous downward flow over the BR at 12 UTC can be observed from the anomalous vertical velocities in the vertical sections (Fig. 10). However, this is the

anomalous flow and the corresponding absolute values (Fig. 12) show that the vertical velocity over the BR is always upward. The time-series plot of the 500-hPa vertical velocity at BR (Fig. 12) shows that the maximum upward flow is at 21 UTC instead of 00 UTC as shown in the four-time-period plots in Figs. 10 and 11. The minimum upward velocity is in the late afternoon between 09 UTC 12 UTC (Fig. 12).

4.1 Diurnal variation of the dynamic fields above the Tibetan Plateau

The time-series plots of the 500-hPa dynamic fields averaged over the central TP region (Fig. 13) show that the vertical velocity over the TP is upward most of the time. The dominant upward motion over the TP can also be observed from the daily-mean field of vertical velocity (Fig. 9b). The strong anomalous downward flow in the early morning at 00 UTC (Figs. 10a, 11a) is almost zero or only slightly downward in the corresponding absolute value (Fig. 13). The maximum upward motion is in the late afternoon between 12 UTC and 15 UTC, which is corresponding to the maximum in precipitation during this period (Fig. 5d).

The 500-hPa divergence over the TP is clearly correlated with the vertical motion over there (Fig. 13). Corresponding to the dominant upward motion over the TP, convergent flow is dominant over there. The slightly divergent flow at 00 UTC also corresponds to the slightly downward flow over the TP. The divergence at UCT00 and the strong convergence at 12 UTC agree well with the corresponding patterns of anomalous divergent and convergent flows over the TP at the 500-hPa level (Fig. 7a, e).

The 500-hPa relative vorticity is always positive over the TP (Fig. 13). The minimum value is at about 06 UTC
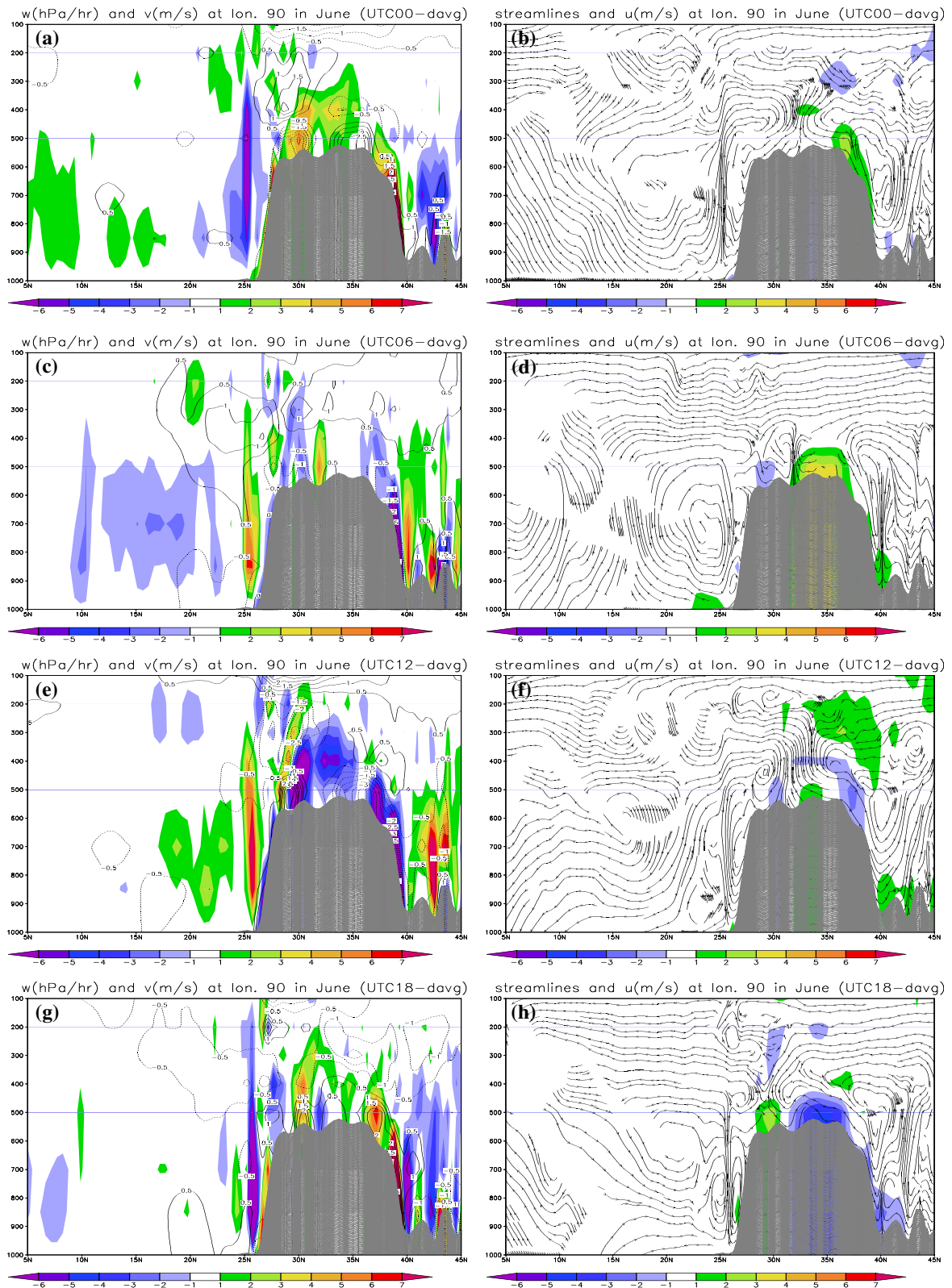
Fig. 10 Diurnal variations (00, 06, 12, 18 UTC minus daily mean) of the flow field in the altitude (hPa)–latitude section at 90°E longitude, averaged in June for the years 1998–2002. **a**, **c**, **e**, **g** Vertical velocity (hPa h^{-1}, *shadings*) and meridional wind (m s^{-1}, *contours*). **b**, **d**, **f**, **k** *Streamlines* and zonal wind (m s^{-1}, *shadings*)
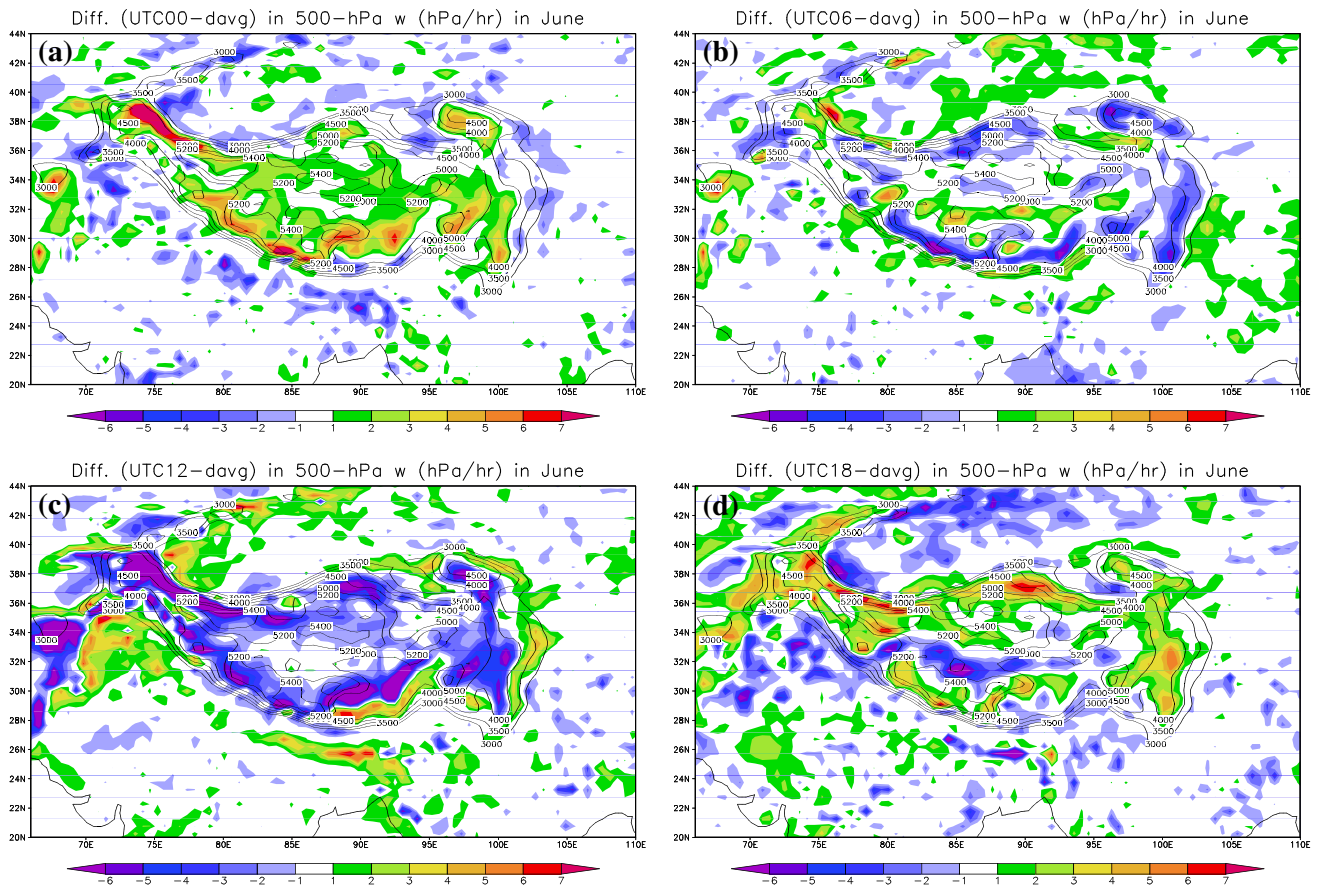
Fig. 11 Diurnal variations (00, 06, 12, 18 UTC minus daily mean) of 500-hPa vertical velocity (hPa h^{-1}, *shadings*) averaged in June for the years 1998–2002. The *contours* show the topography of the Tibetan Plateau above 3,000 m
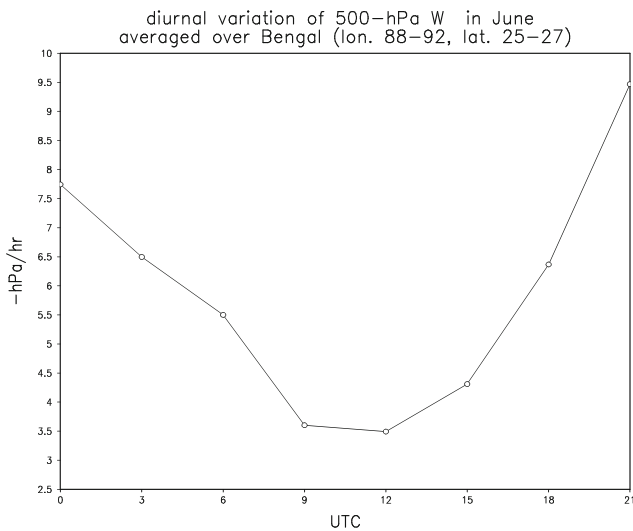

Fig. 12 Diurnal variation of 500-hPa vertical velocity (hPa h^{-1}) in the Bangladesh region (88°–92°E, 25°–27°N) in June for the years 1998–2002

and the maximum value is at about 18 UTC. They are consistent with the anomalous anticyclonic and cyclonic circulations at the 500-hPa level over the TP at the

corresponding periods (Fig. 14a, c). Although the anomalous circulation at 06 UTC is anticyclonic, the actual horizontal flow field is not (Fig. 14b), consistent with the positive relative vorticity at this period (Fig. 13). On the other hand, strong cyclonic circulation can be observed from the actual horizontal flow field at 18 UTC (Fig. 14d). This is also consistent with the maximum 500-hPa relative vorticity over the TP at 18 UTC (Fig. 13).

The variation of the 500-hPa relative vorticity over the TP could be explained by the vorticity equation in isobaric coordinates. Retaining only the high-order terms (Holton 1992), the equation can be written as

$$\frac{d\zeta_a}{dt} \approx -f\nabla \cdot V, \tag{1}$$

where ζ_a is the absolute vorticity, f is the Coriolis parameter, and V is the horizontal velocity vector. At 12 UTC, the 500-hPa convergent flow (negative divergence) over the TP attains the maximum value (Fig. 13) and decreases afterwards. Equation (1) suggests that the rate of change of relative vorticity will decrease with the decrease in convergence. This decrease in the rate of change of vorticity (negative second time derivative) can be observed from the
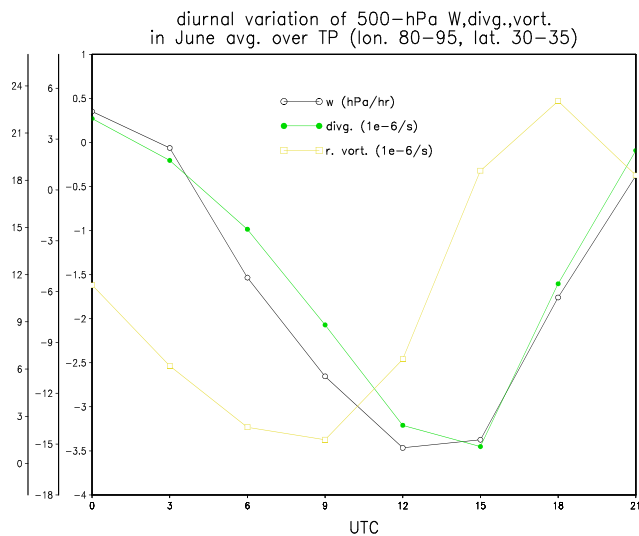
Fig. 13 Diurnal variations of 500-hPa vertical velocity (hPa hr^{-1}, *right vertical axis*), divergence (10^{-6} s^{-1}, *middle vertical axis*), and relative vorticity (10^{-6} s^{-1}, *left vertical axis*) averaged over the central Tibetan Plateau (80°–90°E, 30°–35°N) in June for the years 1998–2002

sinusoidal variation of the 500-hPa relative vorticity over the TP (Fig. 13). After 12 UTC, the slope of the rate of change of relative vorticity starts to decrease and becomes zero at 18 UTC (maximum point) and then negative afterwards. After 03 UTC, the 500-hPa convergent flow over the TP starts increasing (Fig. 13), and consistent with Eq. (1), the rate of change of relative vorticity also increases after 03 UTC. The slope of the rate of change of relative vorticity then increases to zero between 06 UTC and 09 UTC (minimum point) and becomes positive afterwards, and completes the diurnal cycle.

4.2 Possible mechanism of the nocturnal maximum in precipitation over the southern flank of the Tibetan Plateau

It has been discussed in the beginning of this section that the vertical velocity over the BR has a significant diurnal variation in magnitude, with the strongest upward flow at 21 UTC and the weakest upward flow at 12 UTC (Fig. 12).

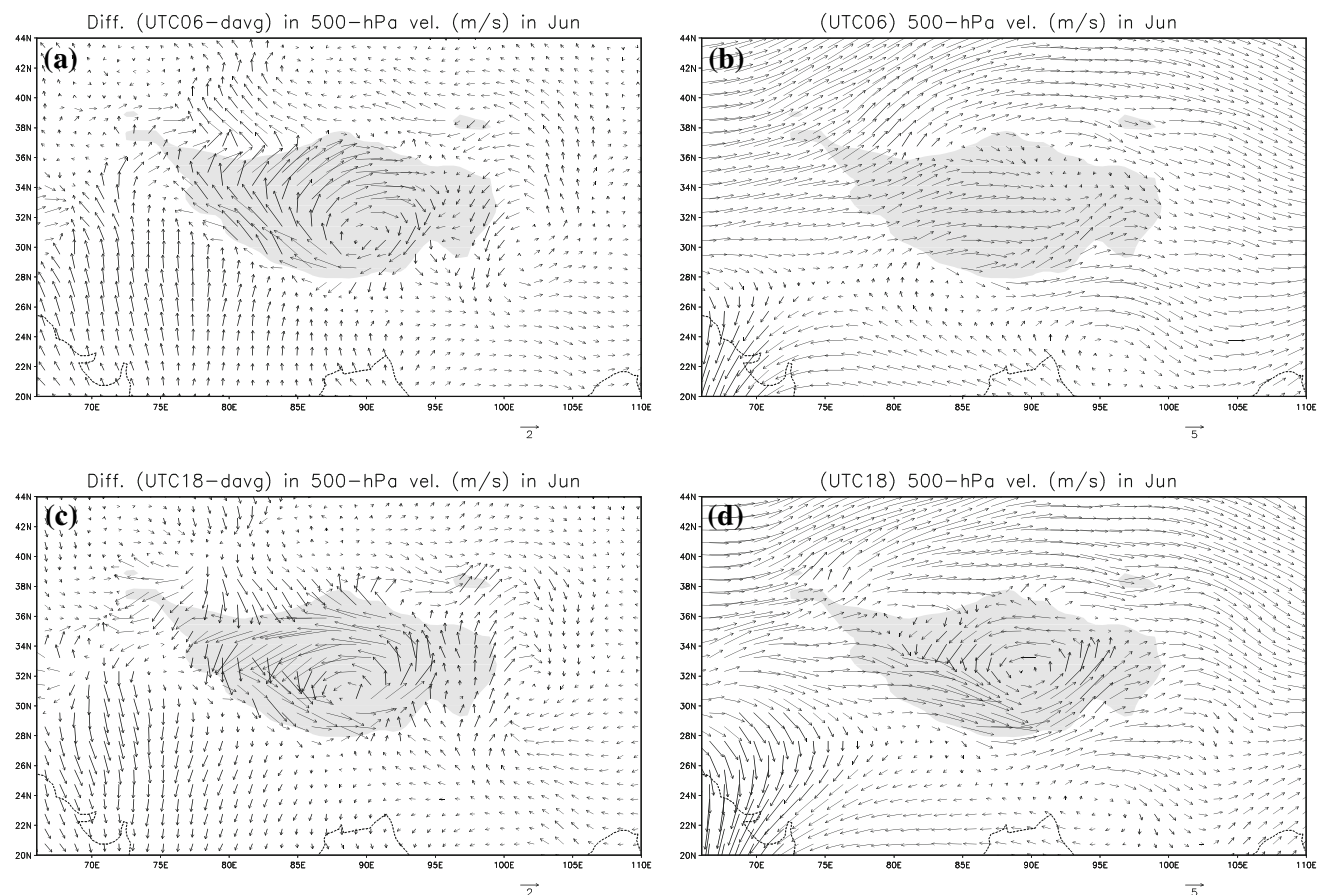**Fig. 14** 500-hPa velocity field (m s^{-1}) at **a**, **b** 06 UTC and **c**, **d** 18 UTC over the Tibetan Plateau in June for the years 1998–2002. **a**, **c** are the differences from the daily mean fields and **b**, **d** are the total fields
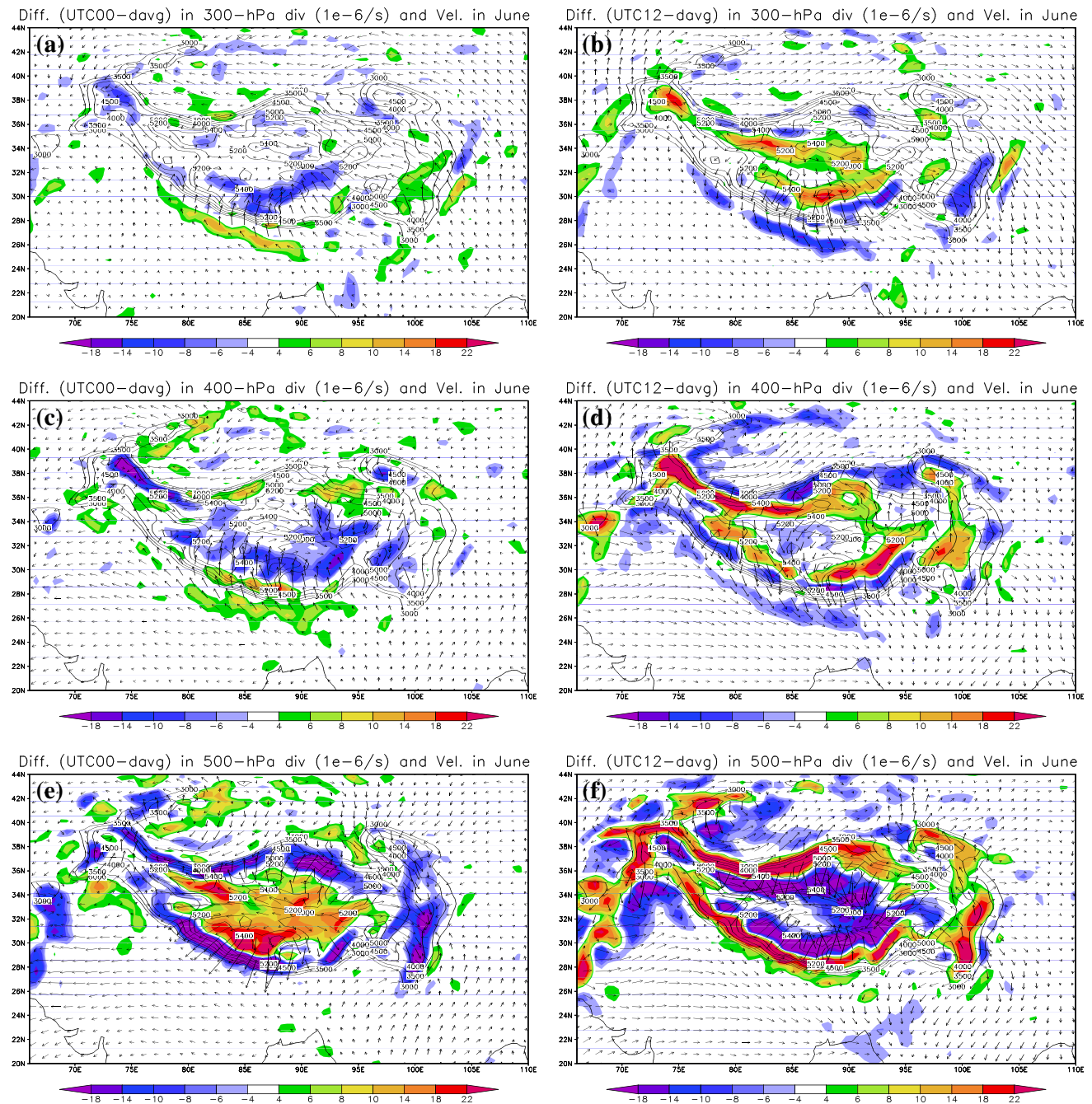
Fig. 15 Diurnal variations (00, 12 UTC minus daily mean) of divergence (10^{-6} s^{-1}, *shadings*) and velocity field (vectors) at levels **a**, **b** 300 hPa, **c**, **d** 400 hPa and **e**, **f** 500 hPa in June for the years 1998–2002. The *contours* show the topography of the Tibetan Plateau above 3,000 m. The scale of the velocity vectors are the same as in Fig. 14

This diurnal variation of upward motion is related to the diurnal variation of the precipitation over the BR. Mechanisms to explain the nocturnal maximum in precipitation over the BR have been proposed in Barros and Lang (2003) and Bhatt and Nakamura (2006). The former study suggested that the change in the magnitude of the upslope flow over the southern slope of the TP may change the location of the maximum precipitation. In the day time the upslope flow is strong and the convergence due to the prevailing southwesterly monsoonal flow at the southern foothill of the TP is weak, and the maximum precipitation is at high elevation up to the southern ridge of the TP. At night, the upslope flow is absent and the convergence due to the prevailing southwesterly monsoonal flow at the southern foothill of the TP is strong and so maximum precipitation is over there. They also suggested the nocturnal precipitation
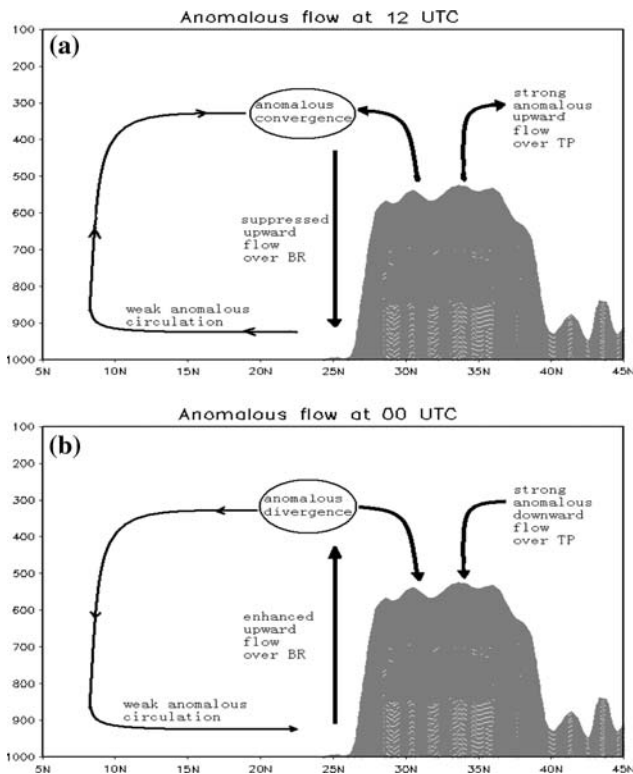
Fig. 16 Schematic diagrams illustrating the proposed mechanism for the diurnal variation of the vertical flow over the BR region at **a** 12 UTC and **b** 00 UTC as discussed in Section 4.2. The cross-sections are altitude (hPa)–latitude sections at longitude 90°E

could be enhanced by the generation of gravity waves. Bhatt and Nakamura (2006) proposed a similar mechanism but they emphasized that the downslope flow at the southern slope of the TP at night time may be the cause of the southward shift of the maximum precipitation from the southern ridge of the TP to the BR.

These are possible mechanisms for explaining the observed nocturnal maximum in precipitation over the BR. However, possibly due to the relatively coarse horizontal resolution of the RCM (60 km), some key features of the above-mentioned mechanisms are not evidenced in the results of the numerical simulations in the present study. First, it appears that the diurnal variation of the vertical velocity is mainly in magnitude but not in position (Fig. 10), and so a change in maximum convergence from the foothill region to the ridge at high elevation as proposed by Barros and Lang (2003) is not observed. Second, there is no downslope flow at the southern slope of the TP in the model results. Even at 00 UTC when the anomalous downslope flow at the southern slope of the TP is at its maximum value (Fig. 10a), the corresponding total flow (figure not shown) is still upslope although the magnitude is small. This is reasonable because the prevailing southwesterly flow of the Indian summer monsoon is strong that

makes the upslope flow prevalent in the southern slope of the TP.

Based on the model results we propose an alternative mechanism to explain the nocturnal maximum of the upward flow and precipitation over the BR. The model results show that the vertical motion over the TP is nearly in opposite phase with the vertical flow over the BR (Figs. 12, 13). When the upward flow over the TP is strong, the upward flow over the BR is weak, and vice versa. This suggests that the diurnal variation in the magnitude of the upward flow over the BR could be associated with the diurnal variation of the vertical motion over the TP. At 12 UTC, the strong anomalous convergence over the TP at 500-hPa level (Fig. 15f) is associated with the strong anomalous divergence over the TP at the upper levels of 300 and 400 hPa (Fig. 15b, d). The anomalous outflow associated with the anomalous divergence at the upper levels results in a band of anomalous convergence in the southern flank of the TP at these levels (Fig. 15d). This band of anomalous convergence in the upper troposphere may suppress the deep upward flow over the BR and so the magnitude of the upward flow over the BR is small at 12 UTC.

On the other hand, at 00 UTC a strong anomalous convergence over the TP at the upper levels (Fig. 15a, c) associated with the strong anomalous divergence over the TP at the 500-hPa level (Fig. 15e) can be observed. Opposite to that at 12 UTC, a band of anomalous divergence at the southern flank of the TP can be observed in the upper levels at 00 UTC (Fig. 15a, c). This band of anomalous divergence is basically caused by the anomalous inflow associated with the anomalous convergence over the TP at the upper levels. This anomalous divergence band at the upper levels favors the strong upward flow over the BR at 00 UTC.

The above proposed mechanism is further illustrated in the schematic diagrams (Fig. 16). This mechanism may explain the maximum and minimum of the vertical motion over the BR at 00 UTC and 12 UTC. However, the discussion of the mechanism is based on the anomalous fields. Recall that in the total flow field the 500-hPa divergence and downward flow over the TP at 00 UTC is very small (Fig. 13), the mechanism does not explain the case at 00 UTC in the real situation. To describe the mechanism for the real situation, it is assumed that without the influence by the vertical motion over the TP, the magnitude of the upward flow over the BR is normally strong. This is basically the case at 00 UTC when the vertical motion over the TP is very weak. As the upward flow over the TP increases and attains the maximum at 12 UTC, the above-discussed mechanism of convergence at the 500-hPa level and divergence at the upper levels over the TP at 12 UTC may explain the reduced upward flow over the BR.

It is interesting to note that the discussed bands of anomalous convergence and divergence at the upper levels at 12 UTC and 00 UTC not only appear in the southern flank of the TP, but can also be observed in the northern flank of the TP at the 400-hPa level (Fig. 15c, d). These bands also appear to be associated with the anomalous vertical motion over the northern foothill of the TP at about 43°N (Fig. 10a, e). However, this is a relatively dry region (Fig. 2b), and so the relevant diurnal variation of precipitation similar to the case in the BR is not significant.

5 Summary and discussions

The present study has investigated the capability of a RCM in simulating the diurnal variation of the Asian summer monsoon precipitation and circulation during the early summer. The model results reveal a synoptic-scale diurnal variation of the circulation over the landmass of the East Asia continent. It appears that the TP plays an important role in the diurnal variation of the circulation in this region. The simulations show that in the middle troposphere (500-hPa level), the diurnal variation of the circulation over the TP is the strongest within the region. Although this mid-tropospheric diurnal forcing over the TP is rather shallow within the 300–500 hPa levels, the strong magnitude of the variation and the large area of the TP could give a significant impact to the circulation in the region. During the late afternoon period (12 UTC), strong convergence at the 500-hPa level in addition to a strong upward motion can be observed over the TP. The weakest vertical motion (weak downward flow) over the TP occurs in the early morning period (00 UTC), accompanied by a very weak divergence over the TP at the 500-hPa level. A significant plateau-scale 500-hPa cyclonic circulation can be observed over the TP at 18 UTC. This cyclonic circulation is basically related to the increase in relative vorticity over the TP, which in turns may be caused by the increase in the 500-hPa convergent flow over the TP during the day time period.

The RCM can simulate reasonably well the patterns of diurnal change in precipitation. The diurnal variation of precipitation over land is generally more significant than that over the oceanic region. This may be related to the larger diurnal variation of surface temperature over the land region. Moreover, there is no diurnal variation of the SST used to run the RCM, and this may be the reason for the weaker diurnal variation of precipitation and circulation simulated by the RCM compared with those from the TRMM and ERA40 data.

The late afternoon maximum of precipitation over the Southeast Asia region such as the Indochina and Malaysian Peninsulas is not well captured by the RCM. The RCM tends to simulate the maximum precipitation in a later period during the midnight. It is possible that the diurnal variation of precipitation over the Southeast Asia region is sensitive to the use of the cumulus parameterization scheme. The sensitivity of the simulated diurnal variation on the use of the cumulus parameterization schemes is a topic worth to be further studied. Apart from the effects of cumulus parameterization schemes, another possibility may be that the spatial resolution of the RCM (60 km in this study) is not fine enough to simulate well the land-sea breeze systems over the Southeast Asia region where the land-sea distribution is complicated. The diurnal variations of precipitation over the Southeast Asia region may be related to the interaction between the systematic monsoon flow and the land-sea breezes over this region (Johnson and Bresch 1991; Ciesielski and Johnson 2006), the effects of coastal mountains (Satomura 2000; Okumura et al. 2003), or gravity waves generated by the diurnal variation of the heat sources over land near the coastal region (Mapes et al. 2003).

The nocturnal maximum in precipitation over the BR in the southern flank of the TP is well captured by the RCM. It has been shown in this study that the nocturnal maximum in precipitation over the southern flank of the TP is associated with the nocturnal maximum in upward motion over the there, which in turns is shown to be significantly influenced by the vertical motion over the TP. The divergence in the upper troposphere associated with the strong upward motion over the TP in the day time may result in a band of convergence in the upper troposphere over the southern flank of the TP. This band of convergence in the upper troposphere tends to produce a downward flow which may suppress the prevailing strong upward motion over the southern flank of the TP. This may be the reason for the less precipitation over the BR in the day time. At night when the upward motion over the TP is weak, the prevailing upward motion over the southern flank of the TP may resume its normal intensity, and thus larger precipitation over the BR occurs at the night time.

Although the results presented in this study are the 5 year simulations of June for the years 1998–2002, it is worth-mentioning that the basic results discussed in this study are also generally true for May, which is also simulated in the same simulations but the results are not presented. In addition, analyses of the TRMM and ERA40 data similar to those presented in Section 3 have been performed (results not shown) for July and August of these 5 years. The results show that the diurnal variations of precipitation and circulation in July and August have similar patterns as those presented in this study for June. In particular, the nocturnal maximum of precipitation over the BR can still be observed. Considering that the TP is a huge elevated heat source in summer (Yanai et al. 1992), it is

likely that the basic results of this study for June have illustrated some climatological features of the diurnal cycle in the summer period over the region.

References

Anthes RA (1977) A cumulus parameterization scheme utilizing a one-dimensional cloud model. Mon Wea Rev 105:270–286

Anthes RA, Hsie EY, Kuo YH (1987) Description of the Penn State/NCAR Mesoscale Model Version 4 (MM4). Tech. Note NCAR/TN-282+STR, NCAR, Boulder, Colo., p 66

Barros A, Lang TJ (2003) Monitoring the monsoon in the Himalayas: observations in central Nepal, June 2001. Mon Wea Rev 131:1408–1427

Bhatt BC, Nakamura K (2005) Characteristics of monsoon rainfall around the Himalayas revealed by TRMM precipitation radar. Mon Wea Rev 133:149–165

Bhatt BC, Nakamura K (2006) A climatological-dynamical analysis associated with precipitation around the southern part of the Himalayas. J Geophy Res 111:D02115. doi:10.1029/2005JD006197

Chan JCL, Liu Y, Chow KC, Ding Y, Lau WKM, Chan KL (2004) Design of a regional climate model for the simulation of south China summer monsoon rainfall. J Meteor Soc Japan 82:1645–1665

Chow KC, Liu Y, Chan JCL, Ding Y (2006) Effects of surface heating over Indochina and India landmasses on the summer monsoon over south China. Int J Climatology 26:1339–1359

Ciesielski PE, Johnson RH (2006) Contrasting characteristics of convection over the northern and southern south China Sea during SCSMEX. Mon Wea Rev 134:1041–1062

Fujinami H, Yasunari T (2001) The seasonal and intraseasonal variability of diurnal cloud activity over the Tibetan Plateau. J Meteor Soc Japan 79:1207–1227

Giorgi F, Marinucci MR, Bates GT (1993a) Development of a second-generation regional climate model (RegCM2). Part I: boundary layer and radiative transfer processes. Mon Wea Rev 121:2794–2813

Giorgi F, Marinucci MR, Bates GT (1993b) Development of a second-generation regional climate model (RegCM2). Part II: convective processes and assimilation of lateral boundary conditions. Mon Wea Rev 121:2814–2832

Hirose M, Nakamura K (2005) Spatial and diurnal variation of precipitation systems over Asia observed by the TRMM precipitation. J Geophy Res 110:D05106. doi:10.1029/2004JD004815

Holton JR (1992) An introduction to dynamic meteorology. Academic Press, New York, p 511

Islam MN, Terao T, Uyeda H, Hayashi T, Kikuchi K, (2005) Spatial and temporal variations of precipitation in and around Bangladesh. J Meteor Soc Japan 83:21–39

Johnson RH, Bresch JF (1991) Diagnosed characteristics of precipitation systems over Taiwan during May-June 1987 TAMEX. Mon Wea Rev 119:2540–2557

Johnson RH, Ciesielski PE, Cotturone JA (2001) Multiscale variability of the atmospheric mixed layer over the western Pacific warm pool. J Atmos Sci 58:2729–2750

Kataoka A, Satomura T (2005) Numerical simulation on the diurnal variation of precipitation over northeastern Bangladesh: a case study of an active period 14–21 June 1995. Sci Online Lett Atmos 1:205–208

Krishnamurti TN, Kishtawal CM (2000) A pronounced continental-scale diurnal mode of the Asian summer monsoon. Mon Wea Rev 128:462–473

Kuo HL, Qian YF (1981) Influence of the Tibetan Plateau on cumulative and diurnal changes of weather and climate in summer. Mon Wea Rev 109:2337–2356

Liu L, Feng J, Chu R, Zhou Y, Ueno K (2002) The diurnal variation of precipitation in monsoon season in the Tibetan Plateau. Adv Atmos Sci 19:365–378

Mapes BE, Warner TT, Xu M (2003) Diurnal patterns of rainfall in northwestern South America. Part III: diurnal gravity waves and nocturnal convection offshore. Mon Wea Rev 131:830–844

Nesbitt SW, Zipser EJ (2003) The diurnal cycle of rainfall and convective intensity according to three years of TRMM measurements. J Climate 16:1456–1475

Nitta T, Sekine S (1994) Diurnal variation of convective activity over the tropical Western Pacific. J Meteor Soc Japan 72:627–641

Ohsawa T, Ueda H, Hayashi T, Watanabe A, Matsumoto J (2001) Diurnal variations of convective activity and rainfall in tropical Asia. J Meteor Soc Japan 79:333–352

Okumura K, Satomura T, Oki T, Khantiyanan W (2003) Diurnal variation of precipitation by moving mesoscale systems: radar observations in northern Thailand. Geophys Res Lett 30(20):2073. doi:10.1029/2003GL018302

Satomura T (2000) Diurnal variation of precipitation over the Indo-China Peninsula: two-dimensional numerical simulation. J Meteor Soc Japan 78:461–475

Tao S, Ding Y (1981) Observational evidence of the influence of the Qinghai Xizang (Tibet) Plateau on the occurrence of heavy rain and severe convective storms in China. J Bull Amer Meteor Soc 62:23–30

Ueno K, Fujii H, Yamada H, Liu L (2001) Weak and frequent monsoon precipitation over the Tibetan Plateau. J Meteor Soc Japan 79:419–434

Yanai M, Li C, Song Z (1992) Seasonal Heating of the Tibetan Plateau and its effects on the evolution of the Asian summer monsoon. J Meteor Soc Japan 70:319–351

Yanai M, Li C (1994) Mechanism of heating and the boundary layer over the Tibetan Plateau. Mon Wea Rev 122:305–323

Yang GY, Slingo J (2001) The diurnal cycle in the tropics. Mon Wea Rev 129:784–801

Yasunari T, Miwa T (2006) Convective cloud systems over the Tibetan Plateau and their impact on meso-scale disturbances in the Meiyu/Baiu frontal zone. A case study in 1998. J Meteor Soc Japan 84:783–803

Zhang J, Lin Z (1992) Climate of China. Wiley, New York. p 376